Whole-exome sequencing reveals *LRP5* mutations and canonical Wnt signaling associated with hepatic cystogenesis

Wybrich R. Cnossen[a], René H. M. te Morsche[a], Alexander Hoischen[b], Christian Gilissen[b], Melissa Chrispijn[a], Hanka Venselaar[c], Soufi Mehdi[d], Carsten Bergmann[e,f], Joris A. Veltman[b], and Joost P. H. Drenth[a,1]

Departments of [a]Gastroenterology and Hepatology and [b]Human Genetics and [c]Center for Molecular and Biomolecular Informatics, Institute for Genetic and Metabolic Disease, Radboud university medical center, 6500 HB Nijmegen, The Netherlands; [d]Department of Digestive and Oncological Surgery, Faculty of Medicine, University Mohammed First, 60000 Oujda, Morocco; [e]Center for Human Genetics, Bioscientia, 55218 Ingelheim, Germany; and [f]Department of Nephrology and Center for Clinical Research, University Hospital Freiburg, 79106 Freiburg, Germany

Polycystic livers are seen in the rare inherited disorder isolated polycystic liver disease (PCLD) and are recognized as the most common extrarenal manifestation in autosomal dominant polycystic kidney disease. Hepatic cystogenesis is characterized by progressive proliferation of cholangiocytes, ultimately causing hepatomegaly. Genetically, polycystic liver disease is a heterogeneous disorder with incomplete penetrance and caused by mutations in *PRKCSH*, *SEC63*, *PKD1*, or *PKD2*. Genome-wide SNP typing and Sanger sequencing revealed no pathogenic variants in hitherto genes in an extended PCLD family. We performed whole-exome sequencing of DNA samples from two members. A heterozygous variant *c.3562C > T* located at a highly conserved amino acid position (p.R1188W) in the *low density lipoprotein receptor-related protein 5* (*LRP5*) gene segregated with the disease (logarithm of odds score, 4.62) but was not observed in more than 1,000 unaffected individuals. Screening of *LRP5* in a PCLD cohort identified three additional mutations in three unrelated families with polycystic livers (p.V454M, p.R1529S, and p.D1551N), again all undetected in controls. All variants were predicted to be damaging with profound structural effects on LRP5 protein domains. Liver cyst tissue and normal hepatic tissue samples from patients and controls showed abundant LRP5 expression by immunohistochemistry. Functional activity analyses indicated that mutant *LRP5* led to reduced wingless signal activation. In conclusion, we demonstrate that germ-line *LRP5* missense mutations are associated with hepatic cystogenesis. The findings presented in this study link the pathophysiology of PCLD to deregulation of the canonical wingless signaling pathway.

gene identification | β-catenin pathway

Polycystic liver diseases (PLD) consist of a group of inherited disorders characterized by abnormal proliferation and differentiation of the bile duct epithelium (1). Ductal plate malformation results in development of multiple fluid-filled cysts spread throughout the liver parenchyma. Progressive hepatic cystogenesis and cyst growth cause hepatomegaly and symptoms such as abdominal distension and pain, pyrosis, anorexia, and dyspnea.

Congenital PLD are clinically heterogeneous, and two major types can be distinguished. Autosomal dominant polycystic kidney disease (ADPKD) is a potentially lethal condition afflicting about 1:400–1:1,000 persons in the United States (2). Patients may develop end-stage renal disease resulting from polycystic kidneys, and 83% have the simultaneous presence of multiple hepatic cysts (3). Formal diagnostic criteria for ADPKD include age, number of renal cysts for each kidney, and family history of renal disease (4, 5). Isolated polycystic liver disease (PCLD) shares the phenotype of a polycystic liver but is distinct from ADPKD because renal disease is absent (6). Some patients may, however, have sporadic renal cysts. Diagnosis of PCLD is made by a family history consistent with autosomal dominant

inheritance and the presence of at least one (<40 y) or more than three (>40 y) hepatic cysts (7).

The natural course of PCLD and ADPKD depends on a spectrum of factors that include age, sex, anticonceptives, pregnancy, and mutation(s) (8–10). Classical linkage analysis has identified four genes that underlie both inherited disorders. Mutations in *polycystic kidney disease 1* or *2* (*PKD1* or *PKD2*) genes (NM_601313 and NM_173910, respectively), which encode polycystin-1 and polycystin-2, are responsible for almost all ADPKD cases (11–13). Both proteins are located in the cilium and are important in renal tubular cell morphogenesis and signaling functions, including the wingless (Wnt) signaling pathway (β-catenin pathway). Mutations in *protein kinase C substrate 80K-H* (*PRKCSH*) and *Saccharomyces cerevisiae homolog 63* (*SEC63*) are linked to PCLD (NM_002743.2 and NM_007214.4, respectively), and both gene products are located to the endoplasmic reticulum and are involved in processing and folding of glycosylated proteins (14–16). In addition, the canonical Wnt signaling may be deregulated by the interaction partner nucleoredoxin of the Sec63 protein during oxidative stress (17). In contrast to ADPKD, only 25% of PCLD cases can be explained by mutations in already known genes (18), indicating that mutations in several other as yet unidentified genes are involved in this disease. We hypothesized that another PCLD gene is involved in an extended PCLD family negative for the known disease genes and performed whole-exome sequencing. This unique approach has proven to be successful for the identification of the genetic cause of other Mendelian disorders (19–21).

Significance

Polycystic liver disease (PCLD) is an autosomal dominantly inherited disorder characterized by multiple fluid-filled hepatic cysts that may cause an extremely enlarged liver. PCLD is genetically heterogeneous, and mutations in *PRKCSH* and *SEC63* are present in ~25% of PCLD patients. This research identifies four unique *LRP5* mutations in four independent families that were all located at highly conserved protein domains. Functional activity analyses suggest that mutant *LRP5* reduces wingless (Wnt) signal activation. This study suggests that imbalanced Wnt signaling is related to hepatic cyst formation.

MEDICAL SCIENCES

Results

Extended Polycystic Liver Disease Family. We assessed a 49-y-old female (III/18) by clinical history taking and physical and radiological examination. She presented to us with a severe symptomatic polycystic liver without renal cysts and complained of abdominal distension, pain, dyspnea, and pyrosis. There was no history of renal disease, hypertension, or intracranial aneurysms. She used contraceptives for a total of 30 y and had two pregnancies. CT scanning revealed numerous cysts with diameters of 5–18 cm in liver segments I–III and VII. Despite aspiration sclerotherapy and laparoscopic deroofing of the liver cysts, her symptoms persisted, and she enrolled in a clinical trial for long-acting octreotide treatment (22). We expanded our clinical analysis and identified a 40-member Dutch family with three generations of early- and late-onset cystogenesis inherited in an autosomal dominant fashion (PCLD-1). Next, we studied 19 individuals with cystogenesis, of which 16 were affected with a polycystic liver according to the Reynolds criteria (5, 7), and three members were affected with renal cysts that came from the 40-member Dutch family (Fig. 1A). The proband (III/18) possessed no pathogenic variants affecting any of the known PCLD or ADPKD genes.

Whole-Exome Sequencing Identifies Pathogenic *LRP5* Variant. We performed exome sequencing on genomic DNA in two members (III/18 and II/18) from the PCLD-1 family with an advanced polycystic liver phenotype (Fig. 1B). Exome capture and sequencing were performed using the Agilent SureSelect target enrichment system with SOLiD4 sequencing. We identified 24,178 and 25,332 genetic variants per proband, respectively (Tables S1 and S2). Variants were annotated by a bioinformatics pipeline as described previously (19, 20). Variant follow-up required the presence of at least five unique variant reads (different start sites), and the variant had to be present in at least 20–80% of all reads suggestive of heterozygous changes in a dominant model of disease. Next, we prioritized variants based on predicted amino acid consequences and overlap with common variation (presence in dbSNP v134 and/or an in-house database containing 1,300 analyzed exomes of predominantly European ancestry). We identified 11 unique nonsynonymous variants present in both affected relatives (Table S3). All 11 variants were tested for segregation in both probands and all other family members by Sanger sequencing. The only private nonsynonymous variant that cosegregated completely with the disease was a missense mutation (*c.3562C > T* with evolutionary conserved amino acid change p.R1188W) located on chromosome 11q13.2 in the *low-density lipoprotein receptor-related protein 5* (*LRP5*) gene (NM_002335.2; Fig. 1 *C* and *D*). We checked sequence coverage and excluded the presence of potential pathogenic variants in the 2 Mb surrounding *LRP5*. All 19 individuals with cystogenesis possessed *LRP5 c.3562C > T* (Table S4 and Fig. S1). Analysis of the sequence data revealed linkage at the *LRP5* locus with the disease with a significant logarithm of odds (LOD) score of 4.62 (Fig. S2). This *LRP5* variant (*c.3562C > T*) was not detected in genome-wide sequence data from the 1000 Genomes Project (23), 6,500 individuals from the National Heart, Lung, and Blood Institute Exome Sequencing Project (24), or exome data from 1,300 individuals of predominantly European ancestry sequenced in-house (19, 20) and excluded by Sanger sequencing in a control set of 1,000 Dutch DNAs of healthy, unrelated individuals. This *LRP5* mutation affected a highly conserved amino acid and was predicted to be damaging by PolyPhen-2, MutPred, and sorting intolerant from tolerant (SIFT) models (Table 1).

LRP5 is a known disease gene causing severe skeletal bone or retinal disorders and is associated with metabolic disease (Fig. S3). Therefore, we actively investigated the possible presence of subtle clinical signs in our family by slit-lamp eye examination. These investigations excluded familial exudative vitreoretinopathy (FEVR) in any of the family members (*SI Text*). We assessed bone density of the lumbar spine and left hip in 13 patients and 9 unaffected relatives. The lumbar T-score was lower in *LRP5* mutation carriers but within the normal range, and no member had a bone density disorder. Routine laboratory testing, including renal parameters, did not reveal differences between individuals with and without the *LRP5* mutation (Table 2). Therefore, other *LRP5*-related disorders were ruled out in this index family.

Additional LRP5 Variants in Polycystic Liver Disease. To confirm our results, we sequenced *LRP5* in a cohort of 150 unrelated PCLD probands without *PRKCSH*, *SEC63,* or *PKD2* gene mutations. We identified two additional PCLD families (one Dutch and one Moroccan) and one Dutch PCLD singleton case with private *LRP5* missense variants. Mutations *c.1360G > A* (p.V454M) and *c.4587G > C* (p.R1529S) segregated with the disease in both families, and unaffected relatives of the singleton case (*c.4651G > A*; p.D1551N) did not carry the mutation (Fig. S4).

Mutation *c.1360G > A* (p.V454M) was present in an 86-y-old polycystic liver patient. Her mutation-positive daughter had
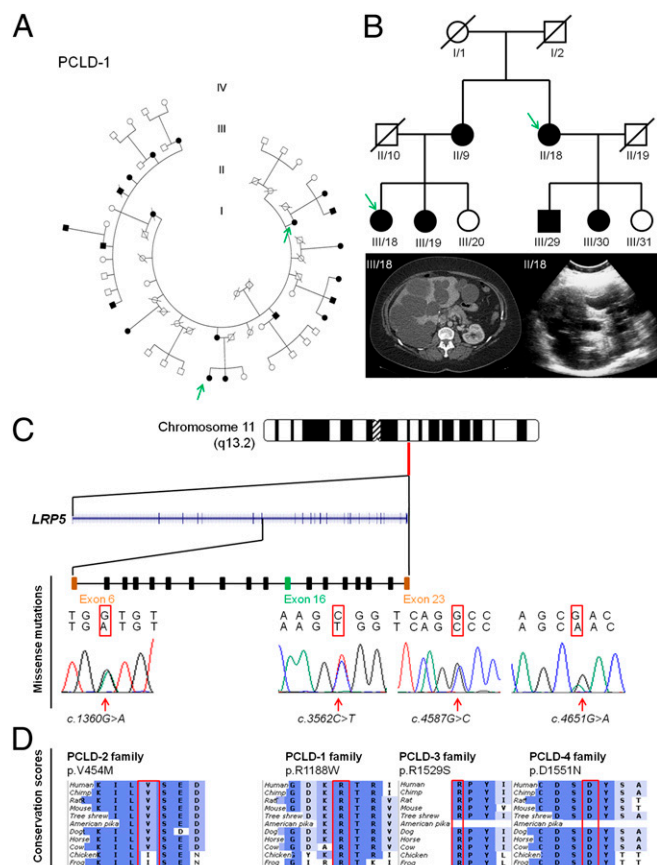

Fig. 1. Identification of *LRP5* variants p.R1188W in an extended Dutch PCLD-1 family (*A*) and three additional *LRP5* variants in three unrelated PCLD families. Generations are denoted with Roman numerals, and individuals are numbered in a counterclockwise way. Squares indicate male sex, and circles indicate female sex. Solid symbols denote affected individuals, and open symbols are individuals without or unknown for PCLD. A slash indicates that the individual is deceased. (*B*) Simplified pedigree from PCLD-1 family with the clinical features by abdominal CT scanning and ultrasound of the liver of both probands (III/18 and II/18) in which whole-exome sequencing was performed (green arrow). (*C*) *LRP5* is located at chromosome 11q13.2, and the sequence electropherogram shows heterozygous germ-line mutations. (*D*) All *LRP5* missense mutations were located at highly evolutionary conserved amino acid regions with ortholog proteins from human to frog.

Table 1. Summary and in silico analysis of four *LRP5* variants in polycystic liver disease

Family ethnicity	Mutation (c.DNA) NM_002335.2	Predicted effect on protein	PolyPhen2	MutPred	SIFT
PCLD-1 Caucasian (Dutch)	c.3562C > T	p.R1188W	Probably damaging 1.00	0.552	Deleterious 0.00
PCLD-2 Caucasian (Dutch)	c.1360G > A	p.V454M	Possibly damaging 0.872	0.520	Deleterious 0.01
PCLD-3 Moroccan	c.4587G > C	p.R1529S	Possibly damaging 0.610	0.288	Deleterious 0.00
PCLD-4 Caucasian (Dutch)	c.4651G > A	p.D1551N	Probably damaging 0.999	0.235	Deleterious 0.00

several bilateral renal cysts and small hepatic cysts on CT scanning. The daughter died as a result of a metastasized liposarcoma at the age of 49. A 43-y-old Moroccan female had multiple dominant hepatic cysts without renal disease. Her 71-y-old mother had several hepatic cysts without renal cysts. Both carried the *c.4587G > C* (p.R1529S) mutation in the *LRP5* gene. A fourth mutation [*c.4651G > A* (p.D1551N)] was present in a 65-y-old male with a polycystic liver and three renal cysts. There was no evidence for renal failure. The phenotype of his deceased parents was unknown, and both his healthy children were without hepatic or renal cysts and did not harbor the *LRP5* mutation. None of the *LRP5* variants were detected in chromosomes from healthy unrelated and ethnically matched controls (Dutch, $n = 1,000$; Moroccan, $n = 525$) nor were they present in the in-house or online exome sequencing datasets. In addition, all four *LRP5* missense variants affected highly conserved amino acids and again were predicted to be damaging or deleterious by PolyPhen-2, MutPred, and SIFT (Table 1).

LRP5 Expression in Liver Cyst Tissues. LRP5 has a wide tissue distribution, including liver and kidney, and expression has been reported in Kupffer cells, macrophages, stellate cells, cholangiocytes, and hepatocytes (25). In line with Northern blotting experiments (26), we found abundant LRP5 protein presence in normal liver tissues and relevant for PCLD. In the affected proband (III/18), we observed intense LRP5 staining of cyst-lining epithelium and bile ducts. The intensity of LRP5 expression was comparable in cyst tissue sections derived from a *PRKCSH* mutant and to bile duct epithelium (Fig. 2 *A* and *B*). This abundant LRP5 expression in cyst tissue indicates that there is no significant loss of structural LRP5 protein from relevant tissue in *LRP5* carriers.

For analysis of structural effects of the *LRP5* variants, we generated separate models for these domains (Fig. 2 *E* and *F* and Table

S5) (27). The human LRP5 protein contains 1,615 amino acids and includes a long extracellular region, a single-span transmembrane region, and a relatively short (208 amino acids) intracellular region. The extracellular region consists of four β-propeller domains with subsequent epidermal growth factor (EGF)-like domains. Near the transmembrane region are three LDL receptor class A repeats, whereas on the cytoplasmatic side, five PPPSP motifs are present. The β-propeller domains all consist of six segments of which most carry a characteristic YWTD motif. Arginine 1188 creates hydrogen bonds and ionic interactions in the core of the β-propeller structure, which is predicted to be lost by the tryptophan mutation (p.R1188W). Additionally, the larger tryptophan side-chain will cause steric clashes, which will most likely disturb the whole β-propeller domain. Valine 454 induces several hydrophobic interactions but is also partly exposed to the solvent. Mutant methionine is predicted not to have major structural effects as both amino acids are hydrophobic, and the methionine side-chain appears to fit at this position (p.V454M). Both p.R1529S and p.D1551N mutations are intracellularly located between PPPSP motifs, and an intracellular homology model is absent.

Reduced Activation of Canonical Wnt Signaling. To identify the underlying mechanism of mutated *LRP5* on the Wnt pathway, we conducted luciferase activity assays with $LRP5_{WT}$, one extracellularly ($LRP5_{R1188W}$) and one intracellularly located ($LRP5_{D1551N}$) mutant, and an empty expression vector as a control. Immunofluorescence imaging in WT and both mutant constructs presented similar localization of LRP5 (Fig. 2 *C* and *D*). Western blots of the cell lysates showed comparable protein expression of all constructs (Fig. 2*G*). Overexpression of the *LRP5* constructs in CHO cells increased basal and Wnt3a-induced luciferase activity compared with the empty vector ($P < 0.0001$). In the presence of Wnt3a, signal

Table 2. Baseline characteristics of PCLD-1 family

Characteristics	No hepatic cystogenesis and no *LRP5* mutation ($n = 9$)	Hepatic cystogenesis and *LRP5* mutation ($n = 13$)	P value
Age (y)	55 ± 12	56 ± 13	NS
Female sex, no. (%)	6 (67)	9 (69)	NS
Bone density: Hip			
T-score	−0.19 ± 0.78	−0.08 ± 0.93	NS
Z-score	0.69 ± 0.68*	0.95 ± 0.94	NS
Bone density: L1-L2-L3-L4			
T-score	1.18 ± 0.95*	0.19 ± 0.88	0.042
Z-score	1.81 ± 0.89*	1.18 ± 1.03	NS
Creatinin (μmol/L)	69 ± 14	73 ± 20	NS
Cholesterol (mmol/L)	5.39 ± 0.71	5.44 ± 1.01	NS
GFR (MDRD) (ml/min/1.73 m^2)	87 ± 13	85 ± 25	NS
BMI (kg/m^2)	25.7 ± 2.5	26.4 ± 5.2	NS
Triglycerides (mmol/L)	1.35 ± 0.71	1.80 ± 0.93	NS
HDL (mmol/L)	1.34 ± 0.40	1.38 ± 0.32	NS
LDL (mmol/L)	3.44 ± 0.82	3.25 ± 0.78	NS
Non HDL (mmol/L)	4.06 ± 0.93	4.07 ± 0.93	NS
HbA1C (%)	5.5 ± 0.6	5.7 ± 0.8	NS
HbA1C (mmol/mol)	37 ± 6	39 ± 9	NS

NS, not significant.
*There was one missing value because of degenerative abnormalities of the lumbar spine in an 85-y-old woman.
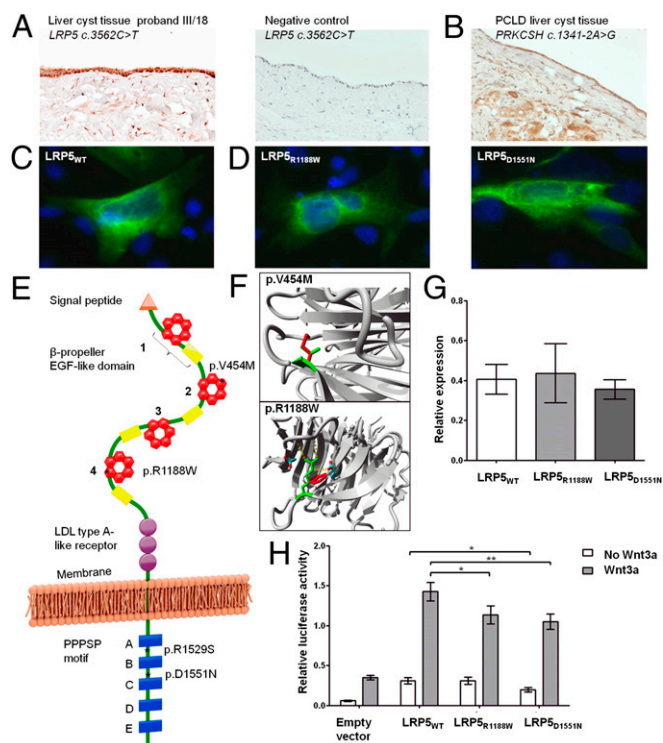
Fig. 2. Functional and structural analyses of LRP5 variants in polycystic liver disease. (*A*) Immunohistochemistry of liver cyst tissue from proband III/18 of PCLD-1 family with *LRP5* mutation *c.3562C > T* (p.R1188W). The cyst lining cholangiocytes present positive staining for LRP5 compared with the negative control next. (*B*) PCLD patient with a *PRKCSH c.1341–2A > G* mutation shows similar staining of liver cyst tissue and expression of LRP5 compared with *A*. (*C*) Localization of LRP5 protein was analyzed by immunofluorescence microscopy. CHO cells were transfected with constructs expressing LRP5$_{WT}$, (*D*) LRP5$_{R1188W}$, or LRP5$_{D1551N}$ and compared with negative controls. No differences in LRP5 localization between all constructs was detected. (*E*) Presentation of the human LRP5 protein and homology modeling of the β-propeller domains highlighting the amino acid changes to emphasize the impact on the configuration and surrounding protein domains. (*F*) Homology modeling of the *LRP5* domains and detailed view of the amino acid changes shows extracellular *LRP5* mutation (*indicated) p.R1188W located at the sixth blade of the fourth β-propeller domain, and *LRP5* mutation p.V454M at the third blade of the second β-propeller domain. Both intracellular mutations p.R1529S and p.D1551N are located between PPPSP motifs A and B and PPPSP motifs B and C, respectively. (*G*) CHO cells were transiently transfected with empty, WT, or mutant *LRP5* vector. Whole cell lysate was analyzed by Western blotting using the V5 antibody and anti–β-actin. LRP5 protein expression levels (normalized to β-actin) are similar between LRP5$_{WT}$ and both mutant constructs LRP5$_{R1188W}$ and LRP5$_{D1551N}$. (*H*) Canonical Wnt signaling activity was analyzed by firefly luciferase activity and normalized to renilla luciferase activity with (in gray) or without addition of 250 ng/mL Wnt3a. All *LRP5* constructs showed a significant increase in Wnt signaling activity compared with the empty vector (*P* < 0.0001). Both *LRP5* mutants showed a decreased Wnt3a-induced signal activity (**P* < 0.001; ***P* < 0.0001). Activity of LRP5$_{D1551N}$ without Wnt3a was significantly decreased compared with LRP5$_{WT}$.

activation was significantly down-regulated by 30% and 45%, taking into account the basal activity in both *LRP5* mutants compared with the LRP5$_{WT}$. We also detected a significant decreased (*P* < 0.001) activity of *LRP5* mutant p.D1551N without the presence of Wnt3a (Fig. 2*H*). Luciferase activity assays were repeated in HEK293 and human liver-derived H69 cells, where comparable significant results were obtained (Fig. S5).

Altered Expression Levels of Wnt Target Genes. Subsequently, we conducted quantitative PCR (qPCR) experiments of transducers and transcription factors associated with the canonical Wnt

signaling. Our analyses show that HEK293 cells transfected with mutant *LRP5* led to altered expression levels of target genes compared with LRP5$_{WT}$ (Fig. S6). There was a significant increased gene expression of transducers adenomatous polyposis coli, glycogen synthase kinase 3β (GSK3β), and leucine-rich repeat-containing G-protein-coupled receptor 5 (LGR5) and transcription factor v-myc avian myelocytomatosis viral oncogene homolog (c-Myc) in LRP5$_{R1188W}$ or LRP5$_{D1551N}$, compared with LRP5$_{WT}$. Similarly, axis inhibitor-1 (AXIN-1), axis inhibitor-2 (AXIN-2), lymphoid enhancer-binding factor 1 (LEF1), SRY-box 9 (SOX9), fibroblast growth factor 18 (FGF18), and cyclin D1 (CCND1) were also up-regulated. In the presence of the extracellular regulator Wnt3a, expression levels of several Wnt signaling components changed (Fig. S7). Decreased expression levels were found for GSK3β, AXIN-1, AXIN-2, LGR5, c-Myc, CCND1, and LEF1 compared with LRP5$_{WT}$ in both mutated *LRP5* constructs. These results are in line with the functional consequences of these *LRP5* mutations as shown with luciferase activity assays (Figs. S8 and S9).

Discussion

This study identifies *LRP5* as a novel gene associated with hepatic cystogenesis in patients clinically diagnosed with PCLD. The initial discovery was made in two affected relatives from an extended Dutch family by exome sequencing (21). A private missense mutation *c.3562C > T* (p.R1188W) in the *LRP5* gene segregated with 18 affected relatives (>40 y), with a significant LOD score of 4.62. These findings are corroborated by the presence of three additional private missense *LRP5* variants in two PCLD families and one PCLD singleton. All unique variants identified in *LRP5* affected highly conserved amino acids and were predicted to be damaging or deleterious. The identification of *LRP5* as a causative gene follows that of *PRKCSH* (15%) and *SEC63* (6%) for isolated polycystic liver disease in a PCLD cohort (18).

LRP5 is a single-span transmembrane protein that acts as a coreceptor with Frizzled protein family members for transducing signals by Wnt proteins. Wnt signaling directs a number of fundamental physiological mechanisms such as cell proliferation, cell polarity, and cell fate determination during embryonic development (28). Until now, *LRP5* variants were linked to a spectrum of Mendelian genetic diseases. *LRP5*-related disorders include autosomal dominant conditions with abnormal bone density, such as endosteal hyperostosis and osteosclerosis (29–32), but also eye disorders such as recessive and dominant forms of FEVR (29, 33, 34). Our findings expand the clinical spectrum of *LRP5*-associated phenotypes because there were no extrahepatic features in patients with *LRP5* mutations in our studies. Specifically metabolic disorders, diabetes mellitus, skeletal bone, and retinal diseases were absent in the index family, and these were not reported for the other three families. We performed specific clinical investigations in extended family 1 and excluded FEVR in individuals with *LRP5* germ-line mutations by slit-lamp eye examination. Bone density measurements ruled out bone diseases in individuals with and without PCLD. Hepatic or renal cystogenesis has not been observed in association with FEVR or with bone diseases.

Why different *LRP5* mutations can result in such a wide spectrum of complex diseases that targets different tissues remains to be determined. LRP5 is detected by Northern blot analysis, immunohistochemistry, and in situ hybridization studies in several tissues including the liver and kidney (25, 26). Until now, *LRP5* mutations were linked to pathological retina or bone development. In the extended PCLD-1 family, we identified the *LRP5 c.3562C > T* mutation in 22 individuals, of which 19 had hepatic and/or renal cystogenesis. Two members were too young (<40 y) to develop hepatic cysts, and one individual is an example of incomplete penetrance. Indeed, there was considerable clinical heterogeneity in affected members without complaints or patients with severe abdominal discomfort in the PCLD-1 family. This clinical heterogeneity has been described in families with

PRKCSH- and *SEC63*-associated PCLD (14, 18), and penetrance of *PRKCSH*-associated PCLD is estimated at ~80%. Intrafamilial phenotypic variability suggests that modifier genes and/or environmental factors play a major role in PCLD disease expression. Similarly, the clinical expression of *LRP5*-associated bone and eye diseases is highly variable (27).

There have been efforts to recapitulate the involvement of *LRP5* mutations in a number of bone and eye disorders in mice. A targeted KO *Lrp5^tm1Jsak*/*Lrp5^tm1Jsak* mouse suffers from unspecified hepatobiliary abnormalities that might implicate phenotypic overlap with our observed human phenotypes (35). Human and mouse LRP5 share a high degree of amino acid identity to coreceptor low density lipoprotein receptor-related protein 6 (LRP6) and have a similar domain structure (36). Furthermore, there has been speculation about functional redundancy between both transmembrane coreceptors of the canonical Wnt signaling pathway (37). The homozygous KO *Lrp6* mouse is embryonic lethal and possesses polycystic kidneys (37) compatible with the ADPKD phenotype. There is further experimental data to suggest that renal cystogenesis in ADPKD is linked to defective canonical Wnt signal transduction. Perturbations of polycystins cause inappropriate levels of β-catenin, and activation and inactivation of the Wnt signaling pathway are reported in different polycystic kidney disease mice models during embryonic or postnatal development (38–42). Our findings provide a direct link between canonical Wnt signaling and polycystic liver disease as Wnt signaling is reduced in mutant *LRP5* compared with WT *LRP5*. A moderate reduction of signaling activity is in line with known *LRP5* missense mutations in retina and bone disorders (43, 44). These observations support a role of an imbalanced canonical and noncanonical Wnt signal transduction in the pathogenesis of *LRP5*-associated polycystic diseases. We speculate that *LRP5,* along with other genes implicated in hepatic cystogenesis, *PKD1, PKD2, PRKCSH,* and *SEC63,* is part of the functional genetic network. Experimental studies have observed that reduced dosage of these gene products, and in particular polycystin-1, is required to cause cyst formation (45, 46).

The identification of *LRP5* associated with hepatic cystogenesis affords a better understanding of the pathophysiology of PCLD. Positivity for immunoreactive LRP5 in cyst epithelium suggests that the protein is structurally intact. Functional assays in three different cell systems indicate that the mutation renders the protein to be less functional and that leads to inhibition of the canonical Wnt signaling (41, 42).

In conclusion, PCLD is a genetically heterogeneous disorder that may be caused by *LRP5* gene mutations. Our results link hepatic cystogenesis to dysregulated canonical Wnt signaling and are in line with data that were generated from ADPKD models (41, 42). Polycystins modulate Wnt signaling during organ development and contribute to hepatic and renal cystogenesis (42, 47, 48). Our study provides evidence that mutations in *LRP5* are related to hepatic cyst development and fuels the hypothesis that canonical Wnt signal transduction is important in polycystic diseases. It is possible that disruption of other (downstream) members of the Wnt signaling pathway may be associated with initiation of hepatic and renal cyst formation.

Materials and Methods

Human Subjects. Ultrasound images of liver and kidneys were acquired using a 3.6-MHz general purpose clinical echo system (Acuson ×150; SiemensAG) equipped with a curved linear array transducer. Blood samples were collected from all 40 subjects, and DNA was extracted from blood leukocytes using the HP-PCR Template Preparation kit (Roche Applied Science). Formalin-fixed paraffin-embedded liver cyst tissue specimens were available from proband III/18 after laparoscopic cyst fenestration. DNA samples from 1,000 Dutch and 525 Moroccan healthy unrelated individuals were used as controls. All subjects provided written informed consent for all investigations. This study was approved by the Medical Ethics Committee of the Radboud university medical center, The Netherlands.

Sanger Sequencing. PCR products of proband III/18 for all exons of the *PRKCSH, SEC63, PKD1,* and *PKD2* genes were analyzed by traditional Sanger sequencing on ABI310 or ABI3100 Genetic Analyzers (Applied Biosystems). Complete sequence analysis for *PKD1* variants was conducted by an experienced Center (Bioscientia). Exon and exon-intron boundaries of *LRP5* were determined using the Genome Bioinformatics Group of University of California, Santa Cruz (UCSC) Genome Browser, and unique primers were designed (Primer3). Heterozygous changes in *LRP5* were detected by high-resolution melting curves (RotorGene-Q; Qiagen) and validated by Sanger sequencing.

Genome-Wide Copy Number Variation Analysis. DNA from whole blood was analyzed on the CytoScanHD, which contains 2.6 million probes (Affymetrix). Hybridizations were performed according to the manufacturer's protocol. Genotype calls and copy number variation analysis were made using Affymetrix Chromosome Analysis Suite v1.2.0.225.

Whole-Exome Sequencing. Exome enrichment was performed using the SureSelect Human All Exon 50-Mb Kit (Agilent), covering ~23,000 genes. Emulsion PCR and bead preparation were made by using the EZbead system according to the manufacturer's instructions followed by SOLiD4 sequencing (Life Technologies). Reads were mapped to the hg19 reference genome using SOLiD Bioscope software v1.3 and annotated as described previously (19, 20). All nonsynonymous variants shared in both affected individuals, absent or with very low frequency in dbSNP, were tested and validated in healthy and affected members of PCLD-1 family for cosegregation by high-resolution melting curve analysis and Sanger sequencing.

Linkage Analysis. We calculated the two-point LOD score for linkage in the extended family using the SuperLink-v1.6 program in EasyLinkage-v5.08 software package. To determine the actual two-point LOD score for the *LRP5* mutation that was detected in this family, the mutation was considered to be a microsatellite marker in close proximity of *LRP5* (D11S4117). An autosomal dominant mode of inheritance was assumed with a penetrance of ~80%, and the disease allele frequency was estimated at 0.0001 (Fig. S2 and SI Text).

Clinical Investigations. Because *LRP5* mutations are associated with bone density disorder, metabolic, and ocular developmental diseases, we performed additional clinical investigations of members from the PCLD-1 family with a clear genotype-phenotype relation. An ophthalmologist (C.E.N.) performed an eye examination by a slit lamp to exclude retinal disorders such as FEVR. At the same time, we analyzed metabolic and renal parameters in blood from these 22 individuals of the PCLD-1 family. We assessed bone density of the lumbar spine and left hip by dual energy X-ray absorptiometry (DXA scan; Hologic Discovery A). Results are reported as T- and Z-scores, which reflect the number of SDs by which a patient's value differs from the mean of a group of young or age-matched normal controls, respectively.

In Silico Analysis and Homology Modeling. We used three computational tools for the prediction of the functional effect of mutational variants (PolyPhen-2, Mutpred, and SIFT). LRP5 protein structure was created by using an LRP6 template as a start homology model and reconstruction by the YASARA& WHAT-IF Twinset. PDB files were available as templates for homology modeling of WD40 domains (β-propeller subdomains) to incorporate the identified extracellularly located *LRP5* mutations. Separate models were visualized for analysis of structural effects by YASARA.

Immunohistochemistry Studies. Formalin-fixed paraffin-embedded liver cyst tissue from proband III/18, four unrelated PCLD patients with *PRKCSH c.1341– 2A > G* mutations, and normal human liver tissue were available for immunohistochemistry studies. Staining intensity for the presence of LRP5 was compared between *LPR5* and *PRKCSH* mutants.

Expression Constructs. Total RNA was isolated from liver tissue using TRIzol Reagent (Invitrogen), and oligodT cDNA was obtained by RT Transcriptor First Strand cDNA synthesis kit (Roche Applied Sciences). Full-length WT *LRP5* was obtained using the Faststart High Fidelity PCR System (Roche). *LRP5* was cloned into the mammalian expression vector pcDNA3.1_V5_His TOPO-TA (Invitrogen) and checked by Sanger sequencing. An extracellularly *c.3562C > T* (p.R1188W) and an intracellularly located *c.4651G > A* (p.D1551N) *LRP5* construct were generated by mutating the pcDNA.LRP5.WT vector using the Quick Change-II-XL Site-Directed Mutagenesis Kit (Agilent Technologies).

Luciferase Activity Assays. We used three cell lines to assess the functional effects of WT and mutant *LRP5.* For the activity assay, 5.0×10^3 CHO cells, 5.0×10^3

MEDICAL SCIENCES

HEK293 cells, and 5.0×10^3 human cholangiocyte 69 (H69) cells per well were seeded in a 96-well plate in triplicate. After 24 h, cells were transiently transfected using X-tremeGeneHD (Roche) with 100 ng *LRP5* construct ($LRP5_{WT}$; $LRP5_{R1188W}$; $LRP5_{D1551N}$) or empty vector and 100 ng of TCF/LEF1 Reporter or 100 ng negative control according to the manufacturers' instructions (Cignal TCF/LEF1 Reporter Assay Kit; Qiagen). Sixteen hours after transfection, medium was replaced by medium with or without 250 ng/mL human Wnt3a (5036-WN; R&D Systems) to initiate Wnt signaling. Cells were cultured for another 24 h, and luciferase activity was detected using the Dual-Glo Luciferase Assay System (Cat. No. E2920; Promega) in an Infin-iteM200-Pro plate reader (Tecan). Firefly luciferase activity was normalized to Renilla luciferase activity for variations in transfection efficiencies. Values are reported as means ± SD. These experiments were conducted in triplicate and performed three times. Western blotting was also performed to analyze possible differences in expression levels between the WT and mutant *LRP5*.

qPCR. We conducted transient transfections of HEK293 cells with *LRP5* constructs as previously described. The signaling was activated by addition of Wnt3a for 24 h. Total RNA was extracted with TRIzol (Invitrogen). Template cDNA was obtained using the iScript cDNA synthesis kit (Biorad). Expression levels of Wnt target genes were assessed twice by qPCR experiments (in triplicate) using the CFX96 real-time detection system (Biorad).

Immunofluorescence Imaging. A total of 4.0×10^4 CHO cells per well were seeded on poly-L-lysine–coated Ø12-mm cover glasses on a 24-well plate and transiently transfected with 100 ng of $LRP5_{WT}$ or mutant *LRP5* construct. After 24 h, medium was refreshed, and cells were cultured for another 24 h followed by paraformaldehyde fixation and immunofluorescence staining.

Statistics. Groups were compared using descriptive statistics and compared by the Student *t* test. Both groups were compared by using the nonparametric Mann–Whitney *U* test. $P < 0.05$ was considered statistically significant. All analyses were calculated by SPSS software v18.0.

1. Strazzabosco M, Somlo S (2011) Polycystic liver diseases: Congenital disorders of cholangiocyte signaling. *Gastroenterology* 140(7):1855–1859.
2. Torres VE, Harris PC (2009) Autosomal dominant polycystic kidney disease: The last 3 years. *Kidney Int* 76(2):149–168.
3. Bae KT, et al.; Consortium for Radiologic Imaging Studies of Polycystic Kidney Disease (CRISP) (2006) Magnetic resonance imaging evaluation of hepatic cysts in early autosomal-dominant polycystic kidney disease: The Consortium for Radiologic Imaging Studies of Polycystic Kidney Disease cohort. *Clin J Am Soc Nephrol* 1(1):64–69.
4. Ravine D, et al. (1994) Evaluation of ultrasonographic diagnostic criteria for autosomal dominant polycystic kidney disease 1. *Lancet* 343(8901):824–827.
5. Pei Y, et al. (2009) Unified criteria for ultrasonographic diagnosis of ADPKD. *J Am Soc Nephrol* 20(1):205–212.
6. Qian Q (2010) Isolated polycystic liver disease. *Adv Chronic Kidney Dis* 17(2):181–189.
7. Reynolds DM, et al. (2000) Identification of a locus for autosomal dominant polycystic liver disease, on chromosome 19p13.2-13.1. *Am J Hum Genet* 67(6):1598–1604.
8. Chapman AB (2003) Cystic disease in women: Clinical characteristics and medical management. *Adv Ren Replace Ther* 10(1):24–30.
9. Van Keimpema L, et al. (2011) Patients with isolated polycystic liver disease referred to liver centres: Clinical characterization of 137 cases. *Liver Int* 31(1):92–98.
10. Gabow PA, et al. (1990) Risk factors for the development of hepatic cysts in autosomal dominant polycystic kidney disease. *Hepatology* 11(6):1033–1037.
11. The European Polycystic Kidney Disease Consortium (1994) The polycystic kidney disease 1 gene encodes a 14 kb transcript and lies within a duplicated region on chromosome 16. *Cell* 77(6):881–894.
12. Mochizuki T, et al. (1996) PKD2, a gene for polycystic kidney disease that encodes an integral membrane protein. *Science* 272(5266):1339–1342.
13. Rossetti S, et al.; CRISP Consortium (2007) Comprehensive molecular diagnostics in autosomal dominant polycystic kidney disease. *J Am Soc Nephrol* 18(7):2143–2160.
14. Drenth JP, te Morsche RH, Smink R, Bonifacino JS, Jansen JB (2003) Germline mutations in PRKCSH are associated with autosomal dominant polycystic liver disease. *Nat Genet* 33(3):345–347.
15. Li A, et al. (2003) Mutations in PRKCSH cause isolated autosomal dominant polycystic liver disease. *Am J Hum Genet* 72(3):691–703.
16. Davila S, et al. (2004) Mutations in SEC63 cause autosomal dominant polycystic liver disease. *Nat Genet* 36(6):575–577.
17. Müller L, Funato Y, Miki H, Zimmermann R (2011) An interaction between human Sec63 and nucleoredoxin may provide the missing link between the SEC63 gene and polycystic liver disease. *FEBS Lett* 585(4):596–600.
18. Waanders E, te Morsche RH, de Man RA, Jansen JB, Drenth JP (2006) Extensive mutational analysis of PRKCSH and SEC63 broadens the spectrum of polycystic liver disease. *Hum Mutat* 27(8):830.
19. Hoischen A, et al. (2010) De novo mutations of SETBP1 cause Schinzel-Giedion syndrome. *Nat Genet* 42(6):483–485.
20. Gilissen C, et al. (2010) Exome sequencing identifies WDR35 variants involved in Sensenbrenner syndrome. *Am J Hum Genet* 87(3):418–423.
21. Gilissen C, Hoischen A, Brunner HG, Veltman JA (2011) Unlocking Mendelian disease using exome sequencing. *Genome Biol* 12(9):228.
22. Chrispijn M, et al. (2013) Everolimus does not further reduce polycystic liver volume when added to long acting octreotide: Results from a randomized controlled trial. *J Hepatol* 59(1):153–159.
23. Abecasis GR, et al.; 1000 Genomes Project Consortium (2010) A map of human genome variation from population-scale sequencing. *Nature* 467(7319):1061–1073.
24. National Institute of Environmental Health Sciences (2012) Environmental Genome Project Exome Variant Server. Available at http://evs.gs.washington.edu/niehsExome/. Accessed September 28, 2012.
25. Figueroa DJ, et al. (2000) Expression of the type I diabetes-associated gene LRP5 in macrophages, vitamin A system cells, and the Islets of Langerhans suggests multiple potential roles in diabetes. *J Histochem Cytochem* 48(10):1357–1368.
26. Hey PJ, et al. (1998) Cloning of a novel member of the low-density lipoprotein receptor family. *Gene* 216(1):103–111.
27. Nikopoulos K, et al. (2010) Overview of the mutation spectrum in familial exudative vitreoretinopathy and Norrie disease with identification of 21 novel variants in FZD4, LRP5, and NDP. *Hum Mutat* 31(6):656–666.
28. Clevers H, Nusse R (2012) Wnt/β-catenin signaling and disease. *Cell* 149(6):1192–1205.
29. Gong Y, et al.; Osteoporosis-Pseudoglioma Syndrome Collaborative Group (2001) LDL receptor-related protein 5 (LRP5) affects bone accrual and eye development. *Cell* 107(4):513–523.
30. Boyden LM, et al. (2002) High bone density due to a mutation in LDL-receptor-related protein 5. *N Engl J Med* 346(20):1513–1521.
31. Little RD, et al. (2002) A mutation in the LDL receptor-related protein 5 gene results in the autosomal dominant high-bone-mass trait. *Am J Hum Genet* 70(1):11–19.
32. Van Wesenbeeck L, et al. (2003) Six novel missense mutations in the LDL receptor-related protein 5 (LRP5) gene in different conditions with an increased bone density. *Am J Hum Genet* 72(3):763–771.
33. Toomes C, et al. (2004) Mutations in LRP5 or FZD4 underlie the common familial exudative vitreoretinopathy locus on chromosome 11q. *Am J Hum Genet* 74(4):721–730.
34. Qin M, et al. (2005) Complexity of the genotype-phenotype correlation in familial exudative vitreoretinopathy with mutations in the LRP5 and/or FZD4 genes. *Hum Mutat* 26(2):104–112.
35. Fujino T, et al. (2003) Low-density lipoprotein receptor-related protein 5 (LRP5) is essential for normal cholesterol metabolism and glucose-induced insulin secretion. *Proc Natl Acad Sci USA* 100(1):229–234.
36. MacDonald BT, Semenov MV, Huang H, He X (2011) Dissecting molecular differences between Wnt coreceptors LRP5 and LRP6. *PLoS ONE* 6(8):e23537.
37. Pinson KI, Brennan J, Monkley S, Avery BJ, Skarnes WC (2000) An LDL-receptor-related protein mediates Wnt signalling in mice. *Nature* 407(6803):535–538.
38. Saadi-Kheddouci S, et al. (2001) Early development of polycystic kidney disease in transgenic mice expressing an activated mutant of the beta-catenin gene. *Oncogene* 20(42):5972–5981.
39. Happé H, et al. (2009) Toxic tubular injury in kidneys from Pkd1-deletion mice accelerates cystogenesis accompanied by dysregulated planar cell polarity and canonical Wnt signaling pathways. *Hum Mol Genet* 18(14):2532–2542.
40. Qian CN, et al. (2005) Cystic renal neoplasia following conditional inactivation of apc in mouse renal tubular epithelium. *J Biol Chem* 280(5):3938–3945.
41. Miller MM, et al. (2011) T-cell factor/β-catenin activity is suppressed in two different models of autosomal dominant polycystic kidney disease. *Kidney Int* 80(2):146–153.
42. Lal M, et al. (2008) Polycystin-1 C-terminal tail associates with beta-catenin and inhibits canonical Wnt signaling. *Hum Mol Genet* 17(20):3105–3117.
43. Mao W, Wordinger RJ, Clark AF (2011) Functional analysis of disease-associated polymorphism LRP5.Q89R. *Mol Vis* 17:894–902.
44. Kiel DP, et al. (2007) Genetic variation at the low-density lipoprotein receptor-related protein 5 (LRP5) locus modulates Wnt signaling and the relationship of physical activity with bone mineral density in men. *Bone* 40(3):587–596.
45. Fedeles SV, et al. (2011) A genetic interaction network of five genes for human polycystic kidney and liver diseases defines polycystin-1 as the central determinant of cyst formation. *Nat Genet* 43(7):639–647.
46. Fedeles SV, Gallagher AR, Somlo S (2014) Polycystin-1: A master regulator of intersecting cystic pathways. *Trends Mol Med*, 10.1016/j.molmed.2014.01.004.
47. Kim E, et al. (1999) The polycystic kidney disease 1 gene product modulates Wnt signaling. *J Biol Chem* 274(8):4947–4953.
48. Gao H, et al. (2010) PRKCSH/80K-H, the protein mutated in polycystic liver disease, protects polycystin-2/TRPP2 against HERP-mediated degradation. *Hum Mol Genet* 19(1):16–24.

Cnossen et al.